

Article

# An Investigation on the $He^-(1s2s^2\ ^2S)$ Resonance in Debye Plasmas

Arijit Ghoshal <sup>1,\*</sup> and Yew Kam Ho <sup>2</sup><sup>1</sup> Department of Mathematics, Burdwan University, Golapbag, Burdwan 713 104, West Bengal, India<sup>2</sup> Institute of Atomic and Molecular Sciences, Academia Sinica, P.O. Box 23-166, Taipei 106, Taiwan; ykho@pub.iams.sinica.edu.tw

\* Correspondence: arijit98@yahoo.com; Tel.: +91-94341-07364

Academic Editor: Kanti M. Aggarwal

Received: 10 December 2016; Accepted: 5 January 2017; Published: 11 January 2017

**Abstract:** The effect of Debye plasma on the  $1s2s^2\ ^2S$  resonance states in the scattering of electron from helium atom has been investigated within the framework of the stabilization method. The interactions among the charged particles in Debye plasma have been modelled by Debye–Huckel potential. The  $1s2s$  excited state of the helium atom has been treated as consisting of a  $He^+$  ionic core plus an electron moving around. The interaction between the core and the electron has then been modelled by a model potential. It has been found that the background plasma environment significantly affects the resonance states. To the best of our knowledge, such an investigation of  $1s2s^2\ ^2S$  resonance states of the electron–helium system embedded in Debye plasma environment is the first reported in the literature.

**Keywords:** electron; helium; Debye plasma; resonance; stabilization method

## 1. Introduction

The effect of screened Coulomb interactions among the charged particles in hot and dense plasmas on the structural and collisional properties of atomic systems is a matter of great interest, because it gives us fundamental information for the interpretation of various phenomena associated with plasma physics, astrophysics, and experiments performed with charged particles [1–9]. In contrary to a free atomic system, screened Coulomb interactions greatly affect the structural and collisional properties, such as shift of the energy levels, spectral line broadening, change in line shapes, depression of ionization potentials, change of transition properties compared to free systems, and line merging phenomena [10]. Red-shifted spectral lines have been experimentally observed in a number of laser-produced plasmas [9].

Screened Coulomb interactions in hot and dense plasmas is the result of the collective effects of correlated many-particle interactions, and in the lowest order particle correlation, it reduces to the Debye–Huckel model of screening, which depends on the temperature and the density of the plasma. In the Debye–Huckel screening model, the interaction between an ion of positive charge  $Z$  and an electron—separated by a distance  $r$ —is given by the Debye–Huckel potential or static screened Coulomb potential (SSCP):

$$V(r) = -(Z/r)e^{-r/\lambda_D} \quad (\text{in a.u.}), \quad (1)$$

where  $\lambda_D$  is the Debye screening length [1].  $\mu = 1/\lambda_D$  is called the plasma screening parameter. It depends on the temperature and the density of the plasma:  $\lambda_D = 1/\mu = [KT_e/4\pi e^2 N_e]^{1/2} = v_T/\omega_p$ , where  $e$  is the electronic charge,  $N_e$  is the plasma-electron density,  $K$  is the Boltzmann constant,  $T_e$  is the electron temperature,  $v_T$  is the thermal velocity, and  $\omega_p$  is the plasma frequency. The interaction potential (1) is adequate only if the ratio of average Coulomb energy and kinetic

energy of the plasma particles (called plasma coupling parameter  $\Gamma$ ) is much less than unity. Such conditions prevail in laser-produced plasmas, EUV, and X-ray laser developments, inertial confinement fusion, astrophysics (stellar atmospheres and interiors), etc. These plasmas are also called weakly coupled plasmas. The densities and temperatures in these plasmas lie in the ranges  $N_e \sim 10^{15}\text{--}10^{18} \text{ cm}^{-3}$ ,  $T_e \sim 0.5\text{--}5 \text{ eV}$  (stellar atmospheres);  $N_e \sim 10^{19}\text{--}10^{21} \text{ cm}^{-3}$ ,  $T_e \sim 50\text{--}300 \text{ eV}$  (laser produced plasmas); and  $N_e \sim 10^{22}\text{--}10^{26} \text{ cm}^{-3}$ ,  $T_e \sim 0.5\text{--}10 \text{ keV}$  (inertial confinement fusion plasmas) [9].

In the present work, we investigate the  $1s2s^2\ ^2S$  resonances in  $He^-$  in Debye plasmas. In particular, the aim of our study is to reveal the plasma screening effects on the resonance parameters. In vacuum, a great deal of experimental and theoretical investigations on  $1s2s^2\ ^2S$  resonance in  $e^- - He$  scattering has appeared in the literature [11–27] (and further references therein). In fact, such a resonance was the first resonance observed in electron–atom scattering [11]. To the best of our knowledge,  $1s2s^2\ ^2S$  resonances in  $He^-$  in Debye plasmas have not been investigated so far, though a great deal of interest in electron scattering from helium in Debye plasma has been shown [28–32] (and further references therein). In the present investigation, to determine resonance parameter, we used the method of model potential within the framework of the stabilization method. Quantities will be expressed in atomic units (a.u.) in the remaining part of this paper, unless explicitly indicated otherwise.

## 2. Method and Calculations

Electron–helium is a four-body system consisting of three electrons and a nucleus, and as such, calculations of resonance parameters for this system are quite involved, even for the pure Coulomb case when correlated wave functions are used [21]. For screened Coulomb cases, when correlated wave functions are used, tackling the full four-body system represents a very challenging effort, and to the best of our knowledge, no such attempt has been made so far. Therefore, instead of solving four-body here, we first reduce it to a three-body problem by the method of model potential. In this method,  $He(1s2s^2\ ^2S)$  is treated as a three-body system consisting of a positive core (nucleus + inner shell electron) and the valence electron going around the core. The interaction between the core and the electron is then modelled by a potential. This interaction potential is constructed in such a manner that it takes care of the effects of both the passive and active electron. Details of the determination of model potentials and their properties are given in references [33–36]. In the literature, many modelled potentials have been presented for the excited states of helium. In the present paper, we use the model potential presented by Varshni [37,38]. Let  $\vec{r}_1$  and  $\vec{r}_2$  be the coordinates of the projectile and the valence electron relative to the core (assumed to be at rest), and  $\vec{r}_{12}$  ( $=\vec{r}_1 - \vec{r}_2$ ) be their relative coordinate. In vacuum, Varshni proposed the following model potential:

$$V_m^{(e^-)}(\vec{r}_2) = -\frac{1}{r_2} \left[ 1 - (1 + \beta r_2)e^{-2\beta r_2} \right] \quad (\text{in a.u.}), \tag{2}$$

where  $\beta$  is a parameter. For  $\beta = 2.601$  and  $\beta = 0.9156$ , it respectively represents the  $He(1s2s\ ^1S)$  and  $He(1s2s\ ^3S)$  configurations. Thus, in Debye plasma,  $V_m^{(e^-)}(\vec{r}_2)$  can be taken as (in a.u.):

$$V_m^{(e^-)}(\vec{r}_2) = -\frac{e^{-r_2/\lambda_D}}{r_2} \left[ 1 - (1 + \beta r_2)e^{-2\beta r_2} \right]. \tag{3}$$

In view of Equation (3), the Hamiltonian of the  $e^- - He(1s2s)$  system embedded in Debye plasma characterized by the Debye–Huckel potential (1) is given by

$$H = -\frac{1}{2}\nabla_1^2 - \frac{1}{2}\nabla_2^2 + V_m^{(e^-)}(\vec{r}_1) + V_m^{(e^-)}(\vec{r}_2) + \frac{e^{-r_{12}/\lambda_D}}{r_{12}}. \tag{4}$$

We determine the resonance parameters by employing stabilization method. This method has been described in detail in previous works [39–42] (and further references therein). So, here we present the implementation only. In order to obtain a stabilization diagram, we choose the following wave function:

$$\Psi(\vec{r}_1, \vec{r}_2) = \sum_{i=1}^N C_i \psi_i = \sum_{i=1}^N C_i (1 + P_{12}) e^{-\alpha(r_1+r_2)} r_1^{l_i} r_2^{m_i} r_{12}^{n_i},$$

$$l_i, m_i, n_i = 0, 1, 2, \dots, l_i \geq m_i, \quad (5)$$

where  $C_i (i = 1, 2, 3, \dots, N)$  are linear expansion coefficients,  $0 < \alpha < 1$  is a scaling parameter, and  $P_{12}$  is the exchange operator such that  $P_{12}f(\vec{r}_1, \vec{r}_2) = f(\vec{r}_2, \vec{r}_1)$  for arbitrary function  $f$ . We expand the summation in the wave function (5) by raising the powers of  $r_1$ ,  $r_2$ , and  $r_{12}$  in such a fashion that the terms corresponding to  $l_i + m_i + n_i = \omega = 0 (N = 1)$  come first, then  $\omega \leq 1 (N = 3)$ ,  $\omega \leq 2 (N = 7)$ , and so on. For a particular value of the Debye length  $\lambda_D$ , employing the wave function (5) in  $H\Psi = E\Psi$ , we obtain the energy levels or stabilization diagram  $E(\alpha)$  ( $0 < \alpha < 1$ ) (as shown in Figure 1a). The emergence of a stabilized or slowly decreasing energy level appears at  $E = E_r$  in the stabilization plateau ensures the existence of a resonance at the energy  $E = E_r$ . Now, to extract the resonance energy  $E_r$  and the resonance width  $\Gamma$ , we must calculate the density of resonance states of the energy levels near the “avoided crossings” with the help of the following formula:

$$\rho_n(E) = \left[ \frac{\alpha_{i+1} - \alpha_{i-1}}{E_n(\alpha_{i+1}) - E_n(\alpha_{i-1})} \right]_{E_n(\alpha_i)=E}, \quad (6)$$

where the index  $i$  is the  $i$ th value for  $\alpha$ , and the index  $n$  is for the  $n$ th resonance. Having calculated the density of resonance states  $\rho_n(E)$  by the above formula, it is fitted to the following Lorentzian form:

$$\rho_n(E) = y_0 + \frac{\Delta}{\pi} \frac{\frac{\Gamma}{2}}{(E - E_r)^2 + \left(\frac{\Gamma}{2}\right)^2}, \quad (7)$$

where  $y_0$  is the baseline offset,  $\Delta$  is the total area under the curve from the base line,  $E_r$  is the centre of the peak, and  $\Gamma$  denotes the full width of the peak of the curve at half height (as shown in Figure 1b). The Lorentzian fitting (7) gives the resonance energy  $E_r$  and resonance width  $\Gamma$ . In the present work, we calculate the densities for each energy level near the avoided crossing and fit with the Lorentzian form (7). Out of all those fittings, the one that gives the best fit (with the least  $\chi$ -square) to the Lorentzian form is considered as the desired results for that particular resonance.

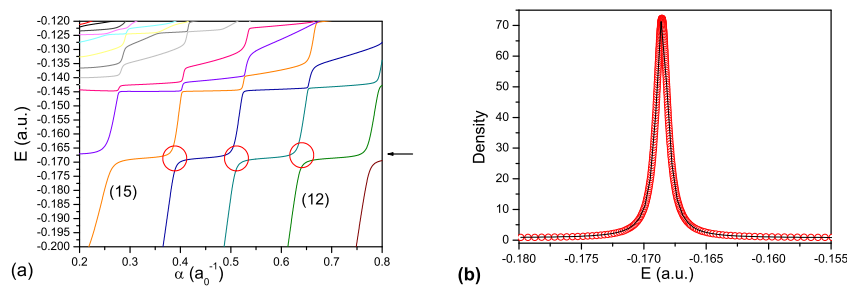


**Figure 1.** (a) Stabilization diagram for  $\mu = 0.0$  obtained by using 525 terms in the wave function (5). The number in parentheses to the right of the solid line indicates the order of appearance of the eigenvalues (energy levels). The arrow shows the position of resonance, and the circles show the point of avoided crossing; (b) The density of resonance states fitted to the Lorentzian form for  $\mu = 0$ . The circles are the calculated values, and the solid line is the fit function. The resonance parameters are determined to be  $E_r = -0.16855$  a.u. and  $\Gamma = 0.00113$  a.u. using the 13th eigenvalue.

### 3. Results and Discussion

The model potential (2) is quite satisfactory for the description of  $He(1s2s\ ^1S)$  and  $He(1s2s\ ^3S)$  configurations. We have computed the eigen energies of  $He(1s2s\ ^1S)$  and  $He(1s2s\ ^3S)$  by solving the corresponding Schrödinger equation within the framework of Ritz's variational principle by employing a wave function of the form:

$$\phi(\vec{r}_2) = \sum_i C_i e^{-a_i r_2} r_2^{l_i}, \quad l_i = 0, 1, 2, \dots, \quad (8)$$

where  $C_i$  is the expansion coefficient and  $a_i$  is a nonlinear variational parameter. For the unscreened case, taking 30 terms in the wave function (8), we have obtained the convergent eigen energies for  $He(1s2s\ ^1S)$  and  $He(1s2s\ ^3S)$  as  $-2.145946$  a.u. and  $-2.175213$  a.u., which are in close agreement with the high precision calculations of G. W. F. Drake [43],  $-2.14597404605442$  a.u. and  $-2.17522937823679$  a.u., respectively.

In Figure 1a, we present stabilization plot  $E(\alpha)$  for  $\mu = 0$ . This diagram has been made using  $N = 525$  ( $\omega = 16$ ) in the wave function (5), and varying the scaling parameter  $\alpha$  within  $[0.2-0.8]$  by giving it an increment of 0.0005. From this figure, we see that a stabilized plateau appears in the diagram around  $-0.168$  a.u. of energy. The positions of avoided crossing are marked with red circles in Figure 1a. We have calculated the density of resonance states near avoided crossings corresponding to each eigenvalue appearing in the stabilization diagram. Those have then been fitted with Lorentzian form. The one for which we obtained the best fit (with the least  $\chi$  square) to the Lorentzian form has been considered as the desired result for that particular resonance. In the present case, fitting corresponding to the 13th eigenvalue gives us the best result, which is shown in Figure 1b. The resonance energy and width are determined as  $E_r = -0.16855$  a.u. and  $\Gamma = 0.00113$  a.u., respectively. It should be mentioned here that we did not consider the energy of the core ( $-2$  a.u.) in our calculation. So, to obtain total resonance energy, we must add the energy of the core. Thus, our calculated resonance energy for  $\mu = 0$  comes out to be  $-2.16855$  a.u.

In Table 1, we show the convergence of our computed results with the increase of the number of terms in the wave function (5) for  $\mu = 0$ . From this table, we note that a convergent result—up to six decimal places—can be obtained by using 525 terms in the wave function. The uncertainty in our results lies on the sixth decimal place. Table 2 also includes the results obtained by using some of the most accurate calculations [15,16,21,22,27]. Comparison indicates that our computed resonance energy is close to the value reported by others, but resonance width differs considerably. For the real three-electron system with final  $^2S$  configuration, the wave function should have three components—the  $(1s)(2s^2)\ ^2S$ ,  $(1s2s)\ ^1S(2s)\ ^2S$ , and  $(1s2s)\ ^3S(2s)\ ^2S$  [21]. In our present approximation, we have only used the  $(1s)(2s^2)\ ^2S$ , and most likely that is the reason for the difference. To include the other two components in our three-body model is not straightforward, and may be an issue of future investigation. Nevertheless, we think that it is still worthwhile to extend our present calculation to the screened environment to see the behaviours of resonance position and width when the screening parameter is changed. We also believe that meaningful values for energy positions and widths of the resonance for the screened cases can be found by considering the ratio—for the unscreened case—between our present results (with three-body wave function) and the earlier results (with four-body wave function) [21].

In Table 2, we present resonance energy and corresponding width for various plasma screening strengths. The same is also presented graphically in Figure 2. From Table 2 and Figure 2, we note that with increasing plasma screening strength, the resonance energy increases, and that the increase is almost linear. However, the width increases slightly at first and starts decreasing steadily. The reason for the decrease of resonance width can be understood if we look at the interaction potential. We note that interaction potentials become weaker with increasing screening strength; as a result, movements of the electrons slow down. This, in turn, makes the lifetime of the resonance process prolonged, and leads to the narrowing of the resonance width, as a consequence of the uncertainty

principle [39]. Furthermore, from Figure 3a, we note that as the screening strength increases, resonance energy approaches toward a bound state of  $He(1s2s^3S)$ . So, the occurrence of pressure ionization might lead (at the limit) to a bound state with zero width [39].

**Table 1.** Resonance energy  $E_r$  (in a.u.) and width  $\Gamma$  (in a.u.) in  $He^-(1s2s^2\ ^2S)$  for  $\mu = 0$ . (a) Method of complex coordinate rotation [21]; (b) R-matrix method [22]; (c) complex stabilization method [27]; (d) experimental results [15]; (e): experimental results [16].

	Results of Present Investigation				Results of Other Investigations				
	$N = 252$ ( $\omega = 12$ )	$N = 308$ ( $\omega = 13$ )	$n = 444$ ( $\omega = 15$ )	$N = 525$ ( $\omega = 16$ )	(a)	(b)	(c)	(d)	(e)
$-E_r$	2.16852	2.16854	2.16855	2.16855	2.19194	2.19171	2.19127	2.19208	2.19204
$\Gamma$	0.001097	0.001129	0.001130	0.001131	0.00041	0.00043	0.00044	0.00041	0.00040

**Table 2.** Resonance energy  $E_r$  (in a.u.) and width  $\Gamma$  (a.u.) in  $He^-(1s2s^2\ ^2S)$  for various values of the screening parameter  $\mu$  (in  $a_0^{-1}$ ) corresponding to  $kT = 4.0$  eV obtained by using the wave function (5).  $E_r^{(e)}$  and  $\Gamma^{(e)}$  denote our estimation as mentioned in the text. The notation  $x[y]$  means  $x \times 10^y$ .

$N_e$ ( $\text{cm}^{-3}$ )	$\mu$	$-E_r$	$\Gamma$	$-E_r^{(e)}$	$\Gamma^{(e)}$
0	0.00	2.16855	0.001131	2.19194	0.0004052
7.82[18]	0.01	2.15858	0.001131	2.18186	0.0004055
3.13[19]	0.02	2.14882	0.001128	2.17200	0.0004043
7.04[19]	0.03	2.13931	0.001120	2.16238	0.0004015
1.25[20]	0.04	2.13006	0.001107	2.15303	0.0003967
1.96[20]	0.05	2.12110	0.001088	2.14398	0.0003901
2.82[20]	0.06	2.11244	0.001064	2.13522	0.0003814
3.83[20]	0.07	2.10409	0.001034	2.12678	0.0003707
5.01[20]	0.08	2.09607	0.000999	2.11868	0.0003581

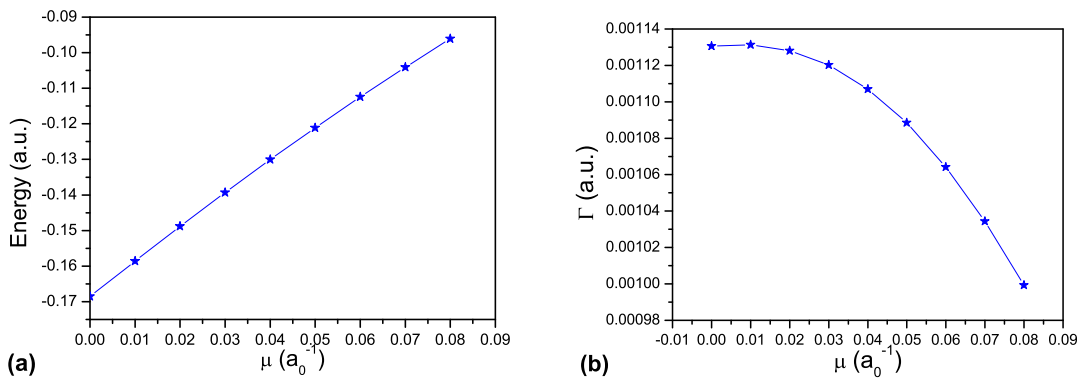


**Figure 2.** (a) Resonance energies  $E_r$  in  $e^- - He(1s2s^2)$  system for different values of the screening parameter  $\mu$ ; (b) Resonance width  $\Gamma$  corresponding to the resonance energies in (a) for different values of the screening parameter  $\mu$  corresponding to  $kT = 4.0$  eV and  $N_e$  in the range  $(0, 5.01 \times 10^{20}) \text{ cm}^{-3}$ .

We have already noticed that our calculated resonance width for the unscreened case differed considerably from the accurate results available in the literature, and that was due to the absence of two other components in the wave function which we employed here. However, as we said earlier, very accurate results (positions and widths of the resonance) for the screened cases can likely be found by considering the ratio (for the unscreened case) between our present results and the earlier results (with four-body wave function) [21]. For the position, this ratio is  $2.191938/2.16855$ , and for the width it is  $0.0004052/0.0011306$ . We multiply our calculated positions and widths for the

screened case by these two ratios to obtain an estimation of positions and widths, respectively, for a screened environment. In Figure 3, we present our estimation of resonance energy  $E_r^{(e)}$  and width  $\Gamma^{(e)}$  with increasing screening effect. Figure 3a also includes the bound state energies of  $He(1s2s\ ^1S)$  and  $He(1s2s\ ^3S)$  with increasing screening effect. Numerical values of the estimation of resonance parameters are also presented in the fifth and sixth columns of Table 2 for the sake of future works relating to this issue. We have calculated those energies using the model potential (3).

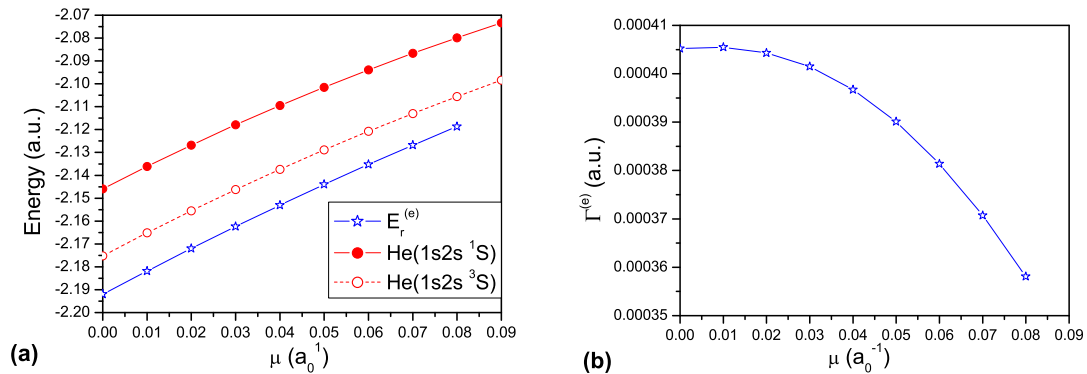


**Figure 3.** (a) Estimated resonance energies (as discussed in the text)  $E_r^{(e)}$  in  $e^- - He(1s2s^2)$  system for different values of the screening parameter  $\mu$ . Shaded circles and hollow circles denote the present calculation of the bound state energies of  $He(1s2s\ ^1S)$  and  $He(1s2s\ ^3S)$ , respectively; (b) Estimated resonance width  $\Gamma^{(e)}$  corresponding to the resonance energies in (a) for different values of the screening parameter  $\mu$  corresponding to  $kT = 4.0$  eV and  $N_e$  in the range  $(0, 5.01 \times 10^{20})$   $cm^{-3}$ .

It should be mentioned that while we have used the stabilization method for resonance calculations in the present work, an alternate method—the complex-scaling (CS) method—has also been used to determine resonance parameters for other systems. The CS method can be easily implemented if the two-body interacting potential is Coulombic; that is, in the form of  $1/r$ . However, the situation becomes more complicated if the two-body interacting potential is a function of  $r$  (instead of just  $1/r$ ), like the model potential we are using here. CS calculations for pure Coulomb cases on model potentials for a positron–Na system and a positron–K system with some approximations have been reported in the literature [44,45]. CS calculations were carried out on a positron–H system with screened Coulomb potentials, where no model potentials are needed [46–48]. However, CS calculations on model potentials in screened Coulomb environments present some challenging problems, and to the best of our knowledge, such calculations have not been reported in the literature. It is worth pursuing this issue further in the future.

#### 4. Conclusions

We have conducted an investigation to determine the effect of Debye plasma on the  $1s2s^2\ ^2S$  resonance states in an electron–helium system by employing the stabilization method. The four-body electron–helium system was reduced to a three-body problem by the method of model potential. This is an added incentive to our present investigation, because otherwise, the determination of the resonance of a four-body system is a tedious and complicated task. Though our present results for the unscreened case do not exactly match with the most accurate results available in the literature due to absence of two components in the wave function, our present investigation—believed to be the first reported in the literature—provides a clear insight into the behaviour of resonance states due to the effect of background plasma. Furthermore, we have presented an estimation of resonance parameters under a plasma environment. We hope that the present investigation will provide fruitful information to research in astrophysics and plasma physics.

**Acknowledgments:** The work was supported by the Ministry of Science and Technology of the ROC. A.G. sincerely acknowledge the support received from UGC through Major Research project (F. No. 43-415/2014(SR)).

**Author Contributions:** The authors have contributed equally to the paper. Both authors have read and approved the final manuscript.

**Conflicts of Interest:** The authors declare no conflict of interest.

## References

1. Margenau, H.; Lewis, M. Structure of Spectral Lines from Plasmas. *Rev. Mod. Phys.* **1959**, *31*, 569–615.
2. Whitten, B.L.; Lane, N.F.; Weisheit, J.C. Plasma-screening effects on electron-impact excitation of hydrogenic ions in dense plasmas. *Phys. Rev. A* **1984**, *29*, 945–952.
3. Nguyen, H.; Koenig, M.; Benredjem, D.; Caby, M.; Coulaud, G. Atomic structure and polarization line shift in dense and hot plasmas. *Phys. Rev. A* **1986**, *33*, 1279–1290.
4. Scheibner, K.; Weisheit, J.C.; Lane, N.F. Plasma screening effects on proton-impact excitation of positive ions. *Phys. Rev. A* **1987**, *35*, 1252–1268.
5. Weisheit, J.C. Atomic excitation in dense plasmas. *Adv. At. Mol. Phys.* **1989**, *25*, 101–131.
6. Salzmann, D. *Atomic Physics in Hot Plasmas*; Oxford University Press: Oxford, UK, 1998.
7. Murillo, M.S.; Weisheit, J.C. Dense plasmas, screened interactions, and atomic ionization. *Phys. Rep.* **1998**, *302*, 1–65.
8. Ichimaru, S. Strongly coupled plasmas: High-density classical plasmas and degenerate electron liquids. *Rev. Mod. Phys.* **1982**, *54*, 1017–1059.
9. Janev, R.K.; Zhang, S.B.; Wang, J.G. A review of quantum collision dynamics in Debye plasmas. *Matter Radiat. Extremes* **2016**, *1*, 237–248.
10. Saha, J.K.; Mukherjee, T.K.; Mukherjee, P.K.; Fricke, B. Effect of strongly coupled plasma on the doubly excited states of heliumlike ions. *Eur. Phys. J. D* **2012**, *66*, 1–9.
11. Schulz, G.J. Resonance in the Elastic Scattering of Electrons in Helium. *Phys. Rev. Lett.* **1963**, *10*, 104–105.
12. Cvejanovic, S.; Comer, J.; Read, F.H. High resolution measurements of the  $2^3S$  cusp and the  $2^2S$  resonance in elastic electron-helium scattering. *J. Phys. B* **1974**, *7*, 468–477.
13. Brunt, J.N.H.; King, G.C.; Read, F.H. Resonance structure in elastic electron scattering from helium, neon and argon. *J. Phys. B* **1977**, *10*, 1289–1301.
14. Kennerly, R.E.; Van Brunt, R.; Gallaher, A.C. High-resolution measurement of the helium  $1s2s^2\ ^2S$  resonance profile. *Phys. Rev. A* **1981**, *23*, 2430–2442.
15. Gopalan, A.; Bommels, J.; Gotte, S.; Landwehr, A.; Franz, K.; Ruf, M.-W.; Hotop, H.; Bartschat, K. A novel electron scattering apparatus combining a laser photoelectron source and a triply differentially pumped supersonic beam target: Characterization and results for the  $He^- (1s2s^2)$  resonance. *Eur. Phys. J. D* **2003**, *22*, 17–29.
16. Buckman S.J.; Clark, C.W. Atomic negative-ion resonances. *Rev. Mod. Phys.* **1994**, *66*, 539–655.
17. Schulz, G.J. Resonances in Electron Impact on Atoms. *Rev. Mod. Phys.* **1973**, *45*, 378–422.
18. Golden, D.E. *Electron and Photon Interactions with Atoms*; Kleinpoppen, H., McDowell, M.R.C., Eds.; Plenum: New York, NY, USA, 1976; p. 639.
19. Andrick, D. The Differential Cross Section of Low Energy Electron-Atom Collisions. *Adv. At. Mol. Phys.* **1973**, *9*, 207–242.
20. Freitas, L.C.G.; Berrington, K.A.; Burke, P.G.; Hibbert, A.; Kingston, A.E.; Sinfailam, A.L. An eleven-state electron-helium scattering calculation. *J. Phys. B* **1984**, *17*, L303.
21. Ho, Y.K.; Yan, Z.C. Calculation of the  $He^- 1s2s^2\ ^2S$  resonance using fully correlated Hylleraas functions. *Phys. Rev. A* **1999**, *59*, R2559.
22. Fon, W.C.; Berrington, K.A.; Burke, P.G.; Kingston, A.E. A 19-state R-matrix investigation of resonances in  $e^- - He$  scattering. I. The resonance widths and positions. *J. Phys. B* **1989**, *22*, 3939–3949.
23. Temkin, A.; Bhatia, A.K.; Bardsley, J.N. Resonance Quasi-Projection Operators: Calculation of the  $^2S$  Autoionization State of  $He^-$ . *Phys. Rev. A* **1972**, *5*, 1663–1671.
24. Davis, B.F.; Chung, K.T. Saddle-point complex-rotation method for the  $(1s2s2s)^2S$  resonance in  $He^-$ , Li I, Be II, and B III. *Phys. Rev. A* **1984**, *29*, 1878–1882.

25. Hazi, A.U. A purely  $L^2$  method for calculating resonance widths. *J. Phys. B* **1978**, *11*, L259.
26. Junker, B.R. Complex-coordinate method.II. Resonance calculations with correlated target-state wave functions. *Phys. Rev. A* **1978**, *18*, 2437–2442.
27. Junker, B.R.; Huang, C.L. Complex-coordinate method. Structure of the wave function. *Phys. Rev. A* **1978**, *18*, 313–323.
28. Khrabrov, A.V.; Kaganovich, I.D. Electron scattering in helium for Monte Carlo simulations. *Phys. Plasmas* **2012**, *19*, 093511.
29. Shigemura, K.; Kitajima, M.; Kurokawa, M.; Toyoshima, K.; Odagiri, T.; Suga, A.; Kato, H.; Hoshino, M.; Tanaka, H.; Ito, K. Total cross sections for electron scattering from He and Ne at very low energies. *Phys. Rev. A* **2014**, *89*, 022709.
30. Konovalov, D.A.; Fursa, D.V.; Bray, I. J-matrix calculation of electron-helium S-wave scattering. II. Single ionization and single excitation. *Phys. Rev. A* **2012**, *86*, 052704.
31. Zammit, M.C.; Fursa, D.V.; Bray, I.; Janev, R.K. Electron-helium scattering in Debye plasmas. *Phys. Rev. A* **2011**, *84*, 052705.
32. Zammit, M.C.; Fursa, D.V.; Bray, I. Electron scattering in a helium Debye plasma. *Chem. Phys.* **2012**, *398*, 214–220.
33. Hart, G.A.; Goodfriend, P.L. Hellmann Pseudopotential Parameters for Atoms with One Valence Electron. *J. Chem. Phys.* **1970**, *53*, 448–449.
34. Cavaliere, P.; Ferrante, G. Model-Potential Theory of Positron-Alkali-Atom Bound States. I: Ground State Energy and Atomic Properties. *Nuovo Cemento* **1973**, *14*, 127–146.
35. Hibbert, A. Model Potentials in Atomic Structure. *Adv. Atom. Mol. Phys.* **1982**, *18*, 309–340.
36. Laughlin, C.; Victor, G.A. Model-Potential Methods. *Adv. At. Mol. Phys.* **1988**, *25*, 163–194.
37. Varshni, Y.P. Comparison of  $1/N$  expansion and shifted  $1/N$  expansion for eigenenergies of an atomic potential. *Phys. Rev. A* **1988**, *38*, 1595–1598.
38. Varshni, Y.P. Spectrum of helium at high pressures. *Eur. Phys. J. D* **2003**, *22*, 229–233.
39. Ghoshal, A.; Ho, Y.K. Doubly excited resonance states of helium in exponential cosine-screened Coulomb potentials. *Phys. Rev. A* **2009**, *79*, 062514.
40. Kar, S.; Ho, Y.K. S-wave resonances in the positron-hydrogen system with screened Coulomb potentials. *J. Phys. B* **2005**, *38*, 3299–3310.
41. Fang, T.K.; Ho, Y.K. Determination of resonance energies and widths of Mg  $3pnl\ ^1D^e$  and  $^1F^o$  doubly excited states by the stabilization method with the B-spline-based configuration interaction approach. *J. Phys. B* **1999**, *32*, 3863–3872.
42. Tan, S.S.; Ho, Y.K. Determination of Resonance Energy and Width by Calculation of the Density of Resonance States Using the Stabilisation Method. *Chin. J. Phys.* **1997**, *35*, 701–707.
43. Drake, G.W.F. *Atomic, Molecular, & Optical Physics Handbook*; AIP Press: New York, NY, USA, 1996; Chapter 11.
44. Umair, M.; Jones, S. Resonances with natural and unnatural parities in positron-sodium scattering. *Phys. Rev. A* **2015**, *92*, 012706.
45. Umair, M.; Jonsell, S. Resonances in positron-potassium  $e^+ - K$  system with natural and unnatural parities. *J. Phys. B* **2016**, *49*, 015004.
46. Chakraborty, S.; Ho, Y.K. Determination of resonance parameters for the  $e^+ - H$  system in Debye plasma environments using the complex-coordinate-rotation method. *Phys. Rev. A* **2008**, *77*, 014502.
47. Ning, Y.; Yan, Z.C.; Ho, Y.K. An investigation of resonances in  $e^+ - H$  scattering embedded in Debye plasma. *Phys. Plasmas* **2015**, *22*, 013302.
48. Ning, Y.; Yan, Z.C.; Ho, Y.K. Natural and Unnatural Parity Resonance States in the Positron-Hydrogen System with Screened Coulomb Interactions. *Atoms* **2016**, *4*, 3.

